Supplementary Information for:

Tuned Thalamic Excitation is Amplified by Visual Cortical Circuits.

Anthony D. Lien and Massimo Scanziani

Neuroscience Graduate Program University of California San Diego, Howard Hughes Medical Institute, Center for Neural Circuits and Behavior, Neurobiology Section and Department of Neuroscience, La Jolla, California 92093-0634, USA

Supplementary Figure 1

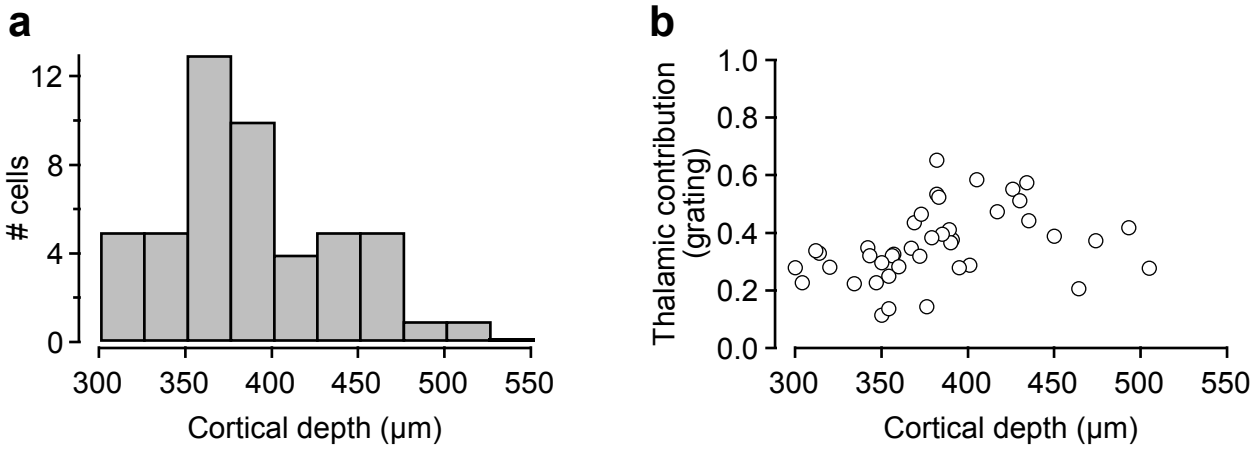

Cortical depth of recorded neurons

a, Distribution of cortical depths for all whole-cell recordings analyzed in the study (n = 49 cells, 40 mice). Note that the study was restricted to cells within a depth range of 300-550 µm corresponding to cortical L4.

b, Thalamic contribution to synaptic excitation during drifting grating plotted against cortical depth for neurons from Figure 1d (n = 42 cells, 33 mice).

Supplementary Figure 2

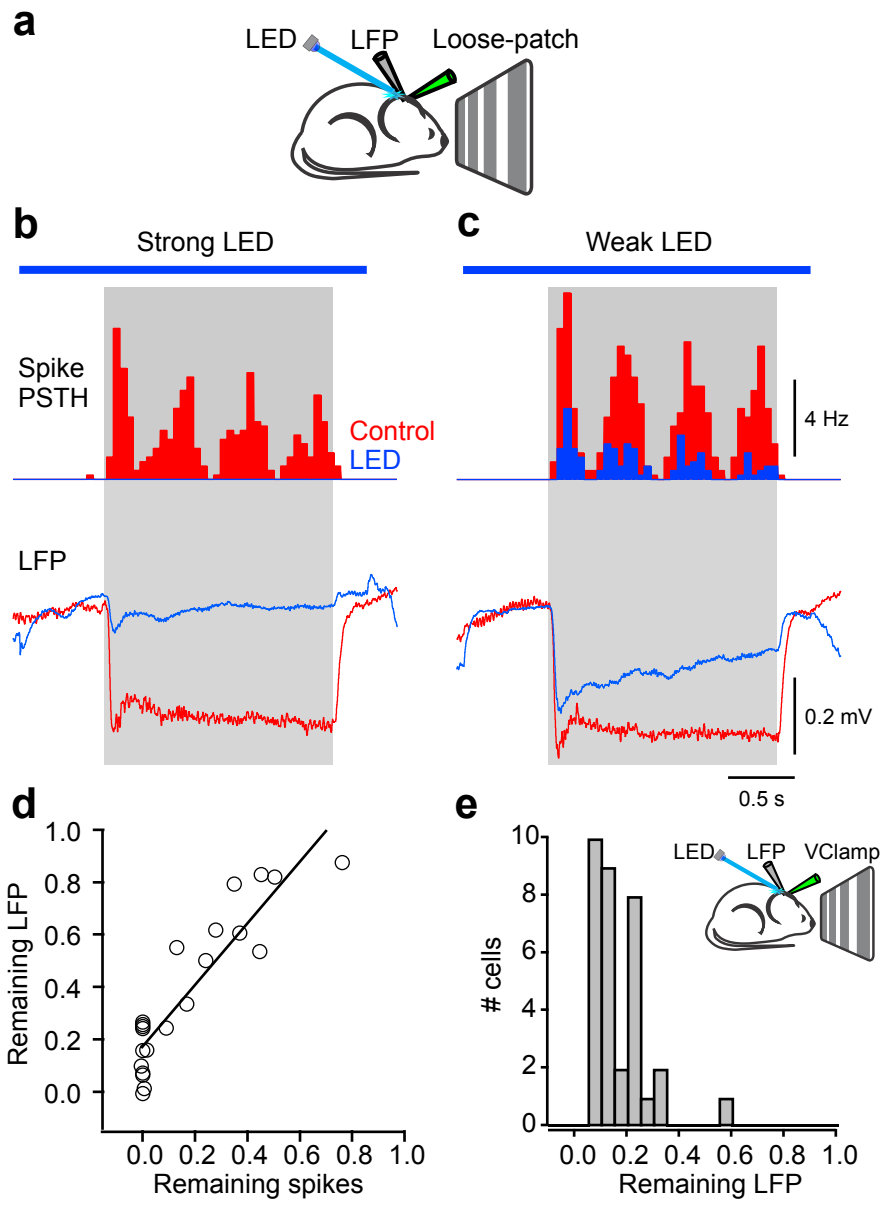

Suppression of the local field potential is correlated with the degree of cortical silencing

a, Schematic of experimental setup. LFP electrode was inserted in L2/3 while loose-patch recordings were made in L4. **b,** Example responses during strong LED illumination (1.3 mW). Top, PSTH of loose-patch recording. Bottom, simultaneously recorded LFP on a second electrode. Red, control trials. Blue, LED trials. PSTH and LFP were averaged across all trials and stimulus directions. **c,** Responses from the same loose-patch and LFP recording in (b) during weak LED illumination (0.2 mW). **d,** The fraction of remaining LFP plotted against the fraction of remaining spikes during LED illumination. (n = 22 cell/LED intensity pairs from 11 cells in 4 animals, LED illumination ranged from < 0.1 mW to 1.3 mW). Black line is a linear fit (remaining LFP = 1.18 x remaining spikes + 0.17, $r^2 = 0.82$). Note that complete cortical silencing reduces the LFP amplitude by ~80%. The remaining LFP likely reflects excitation from the thalamus. **e,** Distribution of remaining LFP during LED illumination for 34/42 neurons from our main drifting grating dataset in which LFP was monitored concurrently with whole-cell recording (schematized in the upper right). The average remaining LFP was 0.16 ± 0.017.

Supplementary Figure 3

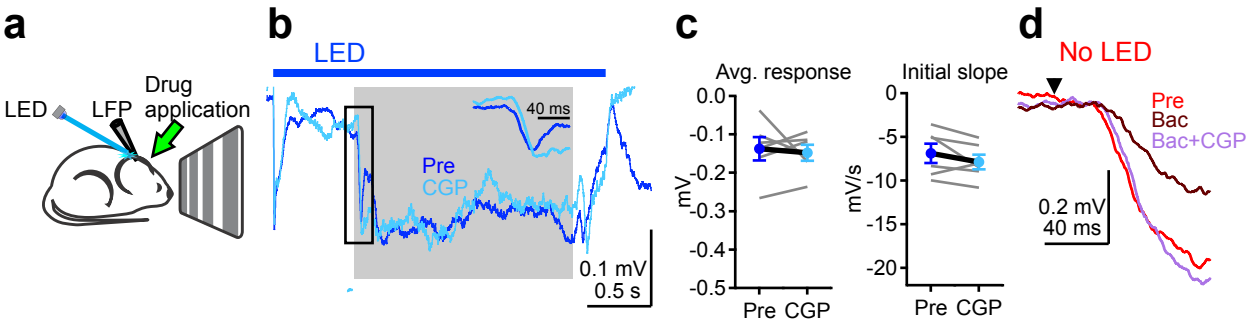

Blocking $GABA_B$ receptors does not affect grating-evoked local field potential during cortical silencing

a, Schematic of experimental setup. To examine whether photostimulation of PV neurons could decrease transmitter release via activation of presynaptic $GABA_B$ receptors on thalamic terminals, we monitored changes in the grating-evoked LFP in L4 during LED illumination 15-45 minutes after application of the $GABA_B$ receptor antagonist CGP54626 (10 µM) to the cortical surface. In these experiments, a full durotomy was performed. **b,** Example grating-evoked LFP responses during LED illumination before (Pre, dark blue) and after CGP54626 application (CGP, light blue). Responses are the avearage across all stimulus directions (36 trials). Inset, expanded view of the boxed region during stimulus onset. Note that CGP54626 had little effect on neither the average response amplitude nor the initial slope at the onset of the response. **c,** Left, Average grating-evoked LFP over the duration of the stimulus (1.7 s) during LED illumination before and after CGP application. Right, initial slope of the first 20 ms of the response as obtained by a linear fit. CGP54626 did not significantly change the size of the average response (Pre: 0.14 ± 0.03 mV; CGP: 0.15 ± 0.02 mV; P = 0.73, n = 6 mice) nor the initial slope (Pre: Pre: -6.9 ± 1.1 mV; Post: -7.9 ± 0.8; P = 0.17, n = 6 mice). **d,** Onset of grating-evoked LFP before drug application (Pre, red), during application of $GABA_B$ agonist baclofen (Bac, dark red; 10 µM), and during application of a mixture of baclofen (10 µM) and CGP54626 (Bac+CGP, light purple). Responses are the average across all stimulus directions (36 trials). Note that baclofen reduces the initial slope by 50% however this effect is reversed by the addition of CGP54626 (Pre: -11.2 mV/s; Bac: -5.4 mV/s; Bac+CGP: -11.7 mV/s). Thus, CGP54626 application in **d** was sufficient to reverse baclofen-mediated activation of GABAB receptors. The minimal effect of CGP54626 observed in **b-c** during LED illumination suggests that under our conditions, the photostimulation of PV cells did not significantly alter transmitter release from thalamic terminals via the activation of presynaptic GABA receptors. Error bars, mean ± s.e.m.

Supplementary Figure 4

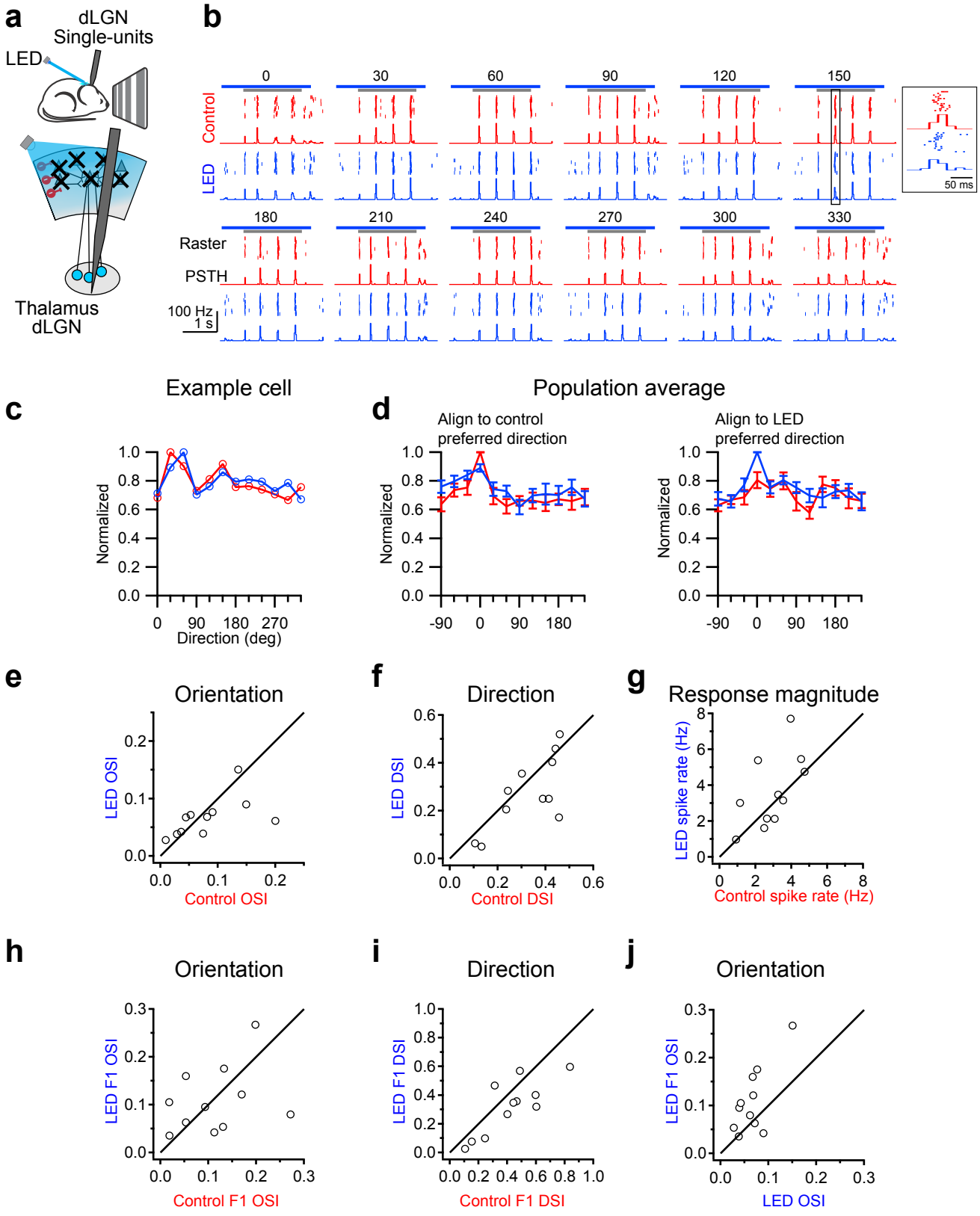

Supplementary Figure 4

Tuning of isolated dLGN units

a, Schematic of experimental setup for recording single units from dLGN with and without cortical silencing. Recordings and photostimulation were performed as previously described (Ref 17). A small craniotomy was performed 2.5 mm posterior of bregma and 2 mm lateral of the midline and a 16-channel linear silicon probe (NeuroNexis a1x16-3mm-50- 177) was inserted to a depth of 2,500-3,300 μm. The probe was coated with DiO to label the recording site, which was confirmed to be in dLGN by post-mortem histology. To activate ChR2-expressing PV cells, the skull over the visual cortex was thinned and a blue (455 nm) fiber-coupled LED (1 mm diameter, Doric Lenses) positioned 5-10 mm illuminated the visual cortex with a power of 25 mW. Spike sorting of single units was performed as previously described (Ref 17). **b,** Spiking responses of a dLGN unit to drifting gratings of various orientations under control (red) and LED-illuminated cortical silencing (blue) conditions. Peri-stimulus time histogram (PSTH) of spiking is displayed below the raster plots. Gray line, visual stimulus (1.7 s). Blue bar, LED illumination (2.6 s). Note the strong F1 modulated spiking at all orientations. Inset, expansion of the grating cycle indicated by the black rectangle. **c,** Orientation tuning curve of the unit in **b** under control (red) and LED (blue) conditions. The response to each orientation was quantified as the average spike rate during the stimulus period. Control and cortical silencing conditions were separately normalized. **d,** Population tuning curves of dLGN single units under control (red) and LED (blue) conditions. Left, Population tuning curves in which control and LED tuning curves for each cell were equally shifted so that the preferred direction under control conditions occurred at 0 degrees. Right, Population tuning curves in which control and LED tuning curves for each cell were equally shifted so that the preferred direction under cortical silencing conditions occurred at 0 degrees. **e,** Orientation selectivity index of the average spike rate (OSI) under control conditions plotted against OSI under LED conditions (control OSI = 0.082 ± 0.02; LED OSI = 0.067 ± 0.01, not significantly different, $p = 0.31$). **f,** Same as **e** for direction selectivity index (control DSI = 0.33 ± 0.04; LED DSI = 0.27 ± 0.05, not significantly different, $p = 0.12$). **g,** Same as **e** for the average response magnitude across all directions (control response = 2.9 ± 0.4 Hz; LED response = 3.6 ± 0.6 Hz; not significantly different, $p = 0.2$). **h-i,** Same as **e-f** for F1 amplitude (control F1 OSI = 0.11 ± 0.024; LED F1 OSI = 0.11 ± 0.021; control F1 DSI = 0.42 ± 0.06; LED F1 DSI = 0.32 ± 0.06). F1 amplitude was determined by fitting the cycle average of the PSTH to a sinusoid at the temporal frequency of the grating (2 Hz). **j,** F1 OSI plotted against OSI of average spike rate during cortical silencing (LED on). Data in **d-j** are from 11 units from 3 mice. Error bars, mean ± s.e.m.

Supplementary Figure 5

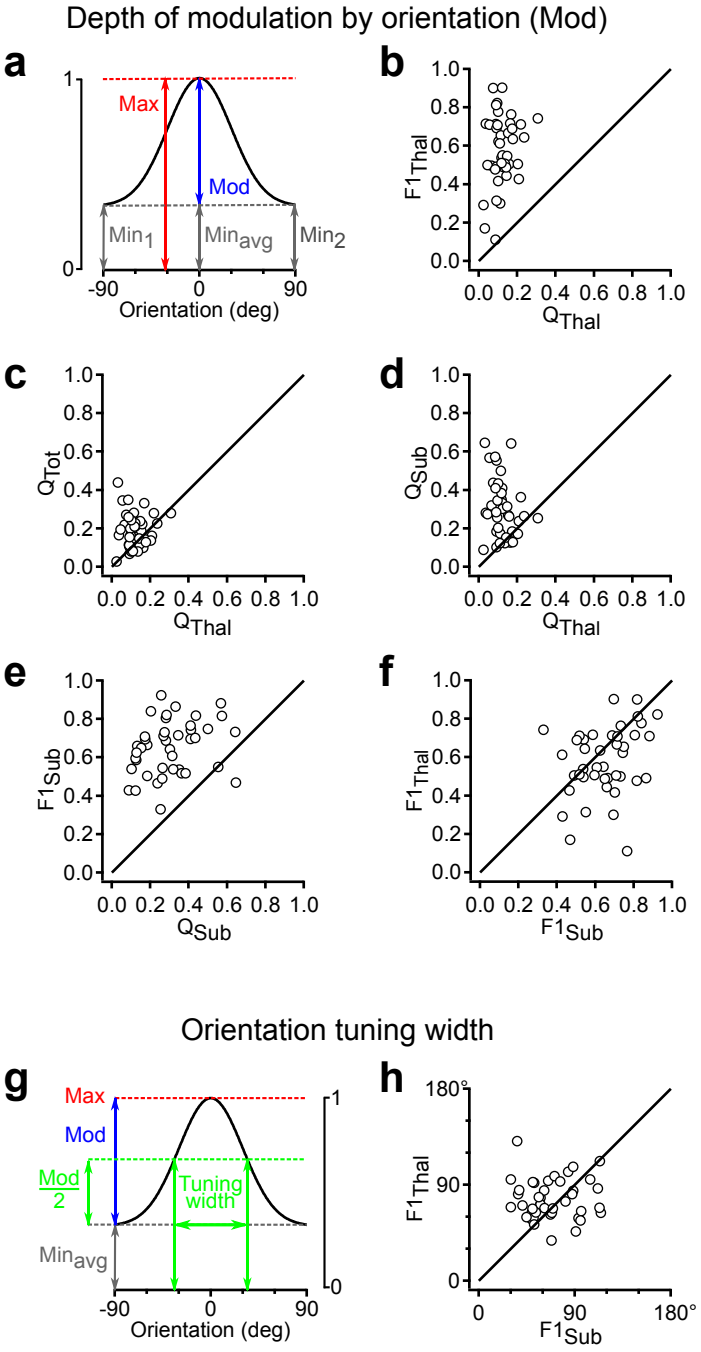

Supplementary Figure 5

Additional measures of orientation tuning

a, Schematic showing how depth of modulation by orientation (Mod) was calculated. For each tuning curve, the responses to opposite directions were averaged together and the tuning curve was circularly shifted so that the orientation producing maximum response was centered at 0 degrees. The tuning curves were then normalized to the maximum response (Max). The minimum values of the tuning curve on either side of the peak (Min_1 and Min_2) were averaged together (Min_{Avg}) and the depth of modulation was calculated as the difference between Max and Min_{Avg}. In most cases, $Min_1 = Min_2 = Min_{Avg}$. Mod ranges from 0 to 1. A value of 0 means that the response at the preferred orientation is the same as that of weakest orientation, 0.5 means that the response at the preferred orientation is half that of the weakest orientation, and 1 means that the response at the weakest orientation is 0. **b-f,** Mod for each OSI scatter plot from the main figures. **b,** Mod $F1_{Thal} = 0.58 \pm 0.03$, Mod $Q_{Thal} = 0.12 \pm 0.01$, significantly different p = 1e-10. **c,** Mod $Q_{Tot} = 0.19 \pm 0.01$, Mod $Q_{Thal} = 0.12 \pm 0.01$, significantly different p = 6e-5. **d,** Mod $Q_{Sub} = 0.3 \pm 0.02$, Mod $Q_{Thal} = 0.12 \pm 0.01$, significantly different p = 3e-8. **e,** Mod $F1_{Sub} = 0.65 \pm 0.02$, Mod $Q_{Sub} = 0.3 \pm 0.02$, significantly different p = 7e-16. **f,** Mod $F1_{Thal} = 0.58 \pm 0.03$, Mod $F1_{Sub} = 0.65 \pm 0.02$, significantly different p = 0.02. **g,** Schematic showing how orientation tuning width was calculated. The orientations at which the tuning curve reached a value of Mod/2 on either side of the peak of the tuning curve were determined by linear interpolation without smoothing. The difference in these two orientations was defined as the tuning width. Because the tuning width has little relevance in the case of tuning curves with very little selectivity, we calculated the tuning width only for $F1_{Thal}$ and $F1_{Sub}$, the parameters that exhibited the strongest tuning. **h,** Tuning width of $F1_{Thal}$ plotted against $F1_{Sub}$. Width of $F1_{Thal} = 76 \pm 3$ degrees, Width of $F1_{Sub} = 68 \pm 4$ degrees, not significantly different p = 0.084; Data in **b-f** and **h** are from n = 42 cells from 33 mice.